Submodule-based Modeling and Simulation of A Series-Parallel Photovoltaic Array Under Mismatch Conditions

Xiangyun Qing, Hao Sun, Xiangsai Feng, C.Y. Chung, *Fellow, IEEE*

***Abstract*—This paper presents a simple and theoretically sound submodule-based model to simulate the characteristics of a PV array with a series-parallel configuration. The proposed model can describe the behavior of bypass diodes as well as the full PV array characteristics under varying irradiance and temperature conditions. Rather than using the non-linear system of equations solved with a Jacobian matrix, separate equations are employed to model the submodule-based PV array, and solved by an easy-to-implement bisection search method. Consequently, the output current of the PV array can be readily determined when its output voltage, the irradiance levels and temperature values of all submodules are given. The robustness and calculation efficiency of the proposed computational method are analyzed. Some test examples allow to exhibit the acceptable accuracy of the proposed model. Special attention of this work is paid to the simulation approach to evaluate the electrical mismatch losses in large-scale PV arrays with nonuniform aging after several years of field operation and exposure.**

***Index Terms*—PV array, Modeling, Bisection method,Partial shading, Mismatch, Submodule**

I. Introduction

The series-parallel (SP) architecture is widely used to large-scale gird-connected photovoltaic (PV) systems for configuration of modules. Ideally, if a PV array works under a uniform irradiance and all cells have an identified current-voltage (I-V) characteristic, most of maximum power point tracking (MPPT) algorithms can detect an unique peak of the power of the PV array. Unfortunately, mismatches arising among different parts of the PV array, are ubiquitous due to manufacturing variances, partial shading, aging, soiling, temperature variations, cell damaging, non-uniform irradiation, etc [1]. As a result, the mismatches will cause power losses of the PV power plant [2]. Power yielded by reversed biased cells should be dissipated in hot spot conditions [3]. Therefore, to make a compromise between high reliability of the PV modules throughout their lifetime and increase on the cost due to the extra p-n junctions, one bypass diode connected in anti-parallel with each group of series connected cells, is utilized externally. A submodule in this context is referred as a group of series connected cells and an anti-paralleled bypass diode serving the group of cells. Although the precaution using the bypass diode in parallel with each submodule can mitigate this mismatch to some extent, the power-voltage (P-V) characteristic of a PV module exhibits more than one peak when the PV cells operate at different illumination levels at mismatch conditions.

Modeling and simulation are the effective techniques commonly used to evaluate the mismatch losses caused by the uniform aging, and to assess the economical feasible of rearranging the modules in the large-scale PV plants after some years of operation. As example, a submodule-based model is suitable for theoretical analysis of efficiency improvement of non-uniformly-aged PV arrays using a PV module reconfiguration strategy without significant investment in [4]. This motivates the development of a new and simple simulation tool allowing submodule-level modeling of partial shading or electrical mismatch in PV arrays.

The electrical behavior of mismatched PV cells in the presence of bypass diodes can data back to the work of Bishop in 1988 in [5]. Although the initial and complete model given in [5] has also been applied and experimentally validated to study the reverse characteristics of shadowed PV cells in [6], parallel combination of bypass diode and series submodule I-V curves is difficult to obtain common voltage values by a simple algebraic calculation, hence, instead by an interpolating procedure. For reducing the computational burden and circumventing the convergence problem when a large PV structure is modeled, the Lambert-W function has been used to express the PV string voltage as an explicit function of its current in [7-10]. However, the term in the Lamber-W function is usually too large, which results in the numerical calculation problem. By modeling the bypass diode as an ideal switch, the concept of the inflection voltage has been introduced to the PV string model with the bypass diodes in [11]. A novel technique to directly relate the power peaks of PV arrays has been presented in [12]. However, only the power peaks are predicted. More recently, a simple relationship equation between I and V for a PV cell has been presented to analyze the characteristics of a PV module under partial shading conditions in [13]. Nevertheless, the simplified equation can lead to the large voltage calculation errors when the current is large. While the submodule-based PV system simulations have been reported in PV*SOL Expert's software documents, the detailed simulation method cannot be publicly available due to some commercial considerations. If the models are formalized by a set of non-linear implicit equations, as shown in [6,7,11,14], the Newton-

X. Qing and H. Sun are with the Department of Automation, East China University of Science and Technology, Shanghai, 200237 China (e-mail: xytsing@ecust.edu.cn; 10141225@mail.ecust.edu.cn).

X. Feng is with the Shanghai Solar Energy Research Center, Shanghai, 201100 China (e-mail:fengxiangsai@solarcell.net.cn)

C.Y. Chung is with the Department of Electrical and Computer Engineering, University of Saskatchewan, Saskatoon, SK, S7N 5A9, Canada (e-mail: c.y.chung@usask.ca)

Manuscript received April 19, 2115; revised August 26, 2115.

Raphson method is usually employed to solve the equations. In this case, the determination and inversion of the Jacobian matrix are the most computationally intensive task. Moreover, a good initial guess point is critical to prevent convergence failures. In addition, the states of bypass diodes are usually failed to judge, as pointed out in [13]. The minimum real root of an equation with higher degree for PV array modeling with the Lambert-W function, as shown in [15], has to be solved. In [16], a method for calculating the strings voltage for a given current value, has been proposed by pre-calculating the complete characteristics of all the strings at a given voltage. Hence, the implementation of this method remains tedious. A comprehensive review can be found in [17].

Based on the bucket effect of maximum short circuit current of the PV submodule, we introduce a submodule-based PV array model using the separate equations in this paper, instead of the nonlinear system of equations usually solved by the Newton-like methods characterized with the Jacobian matrices. The proposed model can describe the behavior of bypass diodes as well as the full PV characteristics under varying irradiance and temperature conditions. The contributions of our work are as follows:

(1) Based on the continuity and monotonicity of the current-voltage function related to the bypass diodes, the bisection method is employed to find the output current of the PV array. Although the bisection method has been applied for the MPPT in [18] and the numerical solution of the nonlinear I-V equation in [19], to the best of our knowledge, we present an application of the bisection method for partial shading conditions for the first time.

(2) We provide a method to evaluate the electrical mismatch losses of the large-scale PV array with nonuniform aging after several years of field operation and exposure. When checking a large amount of PV modules is a non-practical solution for a large-scale PV plant, the degraded electrical parameters and their statistical distributions are obtained from some randomly sampled PV modules. Based on Monte Carlo simulation with these distributions, the proposed method can investigate the benefits of arranging the PV modules using some standard procedures.

(3) We analyze the robustness and calculation efficiency of the proposed computational method. The accuracy of the proposed model is validated by some test examples.

The rest paper is organized as follows. In Section II, we present the submodule-based PV array model under partial shading or mismatch conditions. In section III, we provide a computational method for the submodule-by-submodule PV array simulation. Then, in Section IV, the proposed model is validated by some experimental results, with special attention to the simulation and evaluation of a large-scale PV array under mismatch conditions caused by nonuniform aging. finally, we conclude our work.

II. Modeling

In a SP PV array as shown in Fig.1, N_m PV modules are first connected in series to get a PV string and then N_p PV strings are connected in parallel to construct a PV array. A

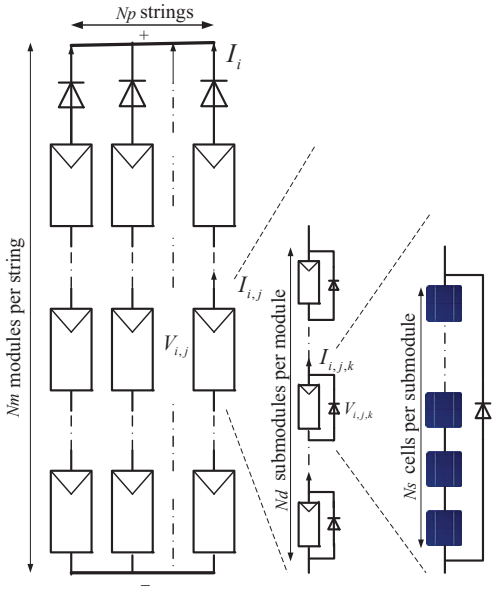

Fig. 1. Series-parallel PV array formed from PV cells.

blocking diode connected in series to one PV string is usually used to block reverse current through the PV string, which is not taken into consideration in this study. Furthermore, a PV module, also known as a PV panel, is composed of N_d series connected submodules. A submodule is made of N_s series-connected cells and one bypass diode (Db) placed in anti-parallel with the cells.

For a PV power generation system, the output voltage value of the PV array is supposed to be specified because it is generally adjusted by the power converter tracking the MPPs. Hence, given its output voltage V_A and the irradiance levels and temperatures of all submodules included to the PV array, its output current I_A should be determined to construct the array I-V characteristics. The PV array current is calculated by a sum of all the PV strings terminal currents, while the the PV array voltage is equal to that the terminal voltage of any PV string. For the i-th PV string with the given output voltage V_i, since the string current I_i is equal to that one of any submodule and the implicit relationship between the submodule current and voltage, the string current I_i can be obtained by numerically solving the equation $F_i(I_i) = 0$, where

$$F_i(I_i) = V_i - \sum_{j=1}^{N_m} \sum_{k=1}^{N_d} V_{i,j,k}(I_{i,j,k}) \tag{1}$$

and $V_{i,j,k}$ is the terminal voltage of the k-th submodule of the j-th PV module contained in the i-th PV string, which is the nonlinear function of the current $I_{i,j,k}$ flowing through the submodule. Each submodule has three elementary flag numbers, as the subscript, that determine uniquely its configuration information in the PV array: the first flag denotes the specific PV string that contains the submodule, the second flag the specific PV module and the third flag the submodule [20]. Obviously, $I_{i,j,k} = I_{i,j} = I_i$, where $I_{i,j}$ is the current flowing through the the j-th PV module contained in the i-th PV string.

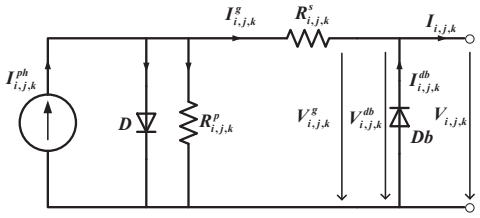

Fig. 2. Equivalent circuit of the submodule.

The circuit model of the the k-th submodule of the j-th PV module contained in the i-th PV string is given in Fig.2. The group of N_s series-connected cells in the submodule is electrically modeled by the most widely used single-diode circuit (or five-parameter model):

$$I^g_{i,j,k} = I^{ph}_{i,j,k} - I^0_{i,j,k}(e^{\frac{V^g_{i,j,k}+R^s_{i,j,k}I^g_{i,j,k}}{N_s V^t_{i,j,k}(T_{i,j,k})A_{i,j,k}}} - 1) - \frac{V^g_{i,j,k}+R^s_{i,j,k}I^g_{i,j,k}}{R^p_{i,j,k}} \quad (2)$$

In (2), terms $I^{ph}_{i,j,k}$, $I^0_{i,j,k}$, $A_{i,j,k}$, $R^s_{i,j,k}$, $R^p_{i,j,k}$ are the five parameters of the model. $V^g_{i,j,k}$, $I^g_{i,j,k}$ are the terminal voltage and current of the group, respectively. $V^t_{i,j,k}(T_{i,j,k})$ is the junction thermal voltage at the temperature $T_{i,j,k}$ (in Kelvin) of the p-n junction

$$V^t_{i,j,k}(T_{i,j,k}) = \frac{k \cdot T_{i,j,k}}{q} \quad (3)$$

where q is the electron charge ($1.60217646\times10^{-19}C$), k is the Boltzmann constant ($1.3806503\times10^{-23}J/K$). The relationship of model parameters analytically as functions of PV irrandiance $G_{i,j,k}$ and temperature $T_{i,j,k}$, is shown in our previous work [21].

By using Kirchhoff voltage and current laws, the relation between the current $I_{i,j,k}$ and voltage $V_{i,j,k}$ of the submodule is given as the following equations:

$$I_{i,j,k} = I^g_{i,j,k} + I^{db}_{i,j,k}, \quad (4)$$

$$V_{i,j,k} = V^{db}_{i,j,k} = V^g_{i,j,k} \quad (5)$$

The relation between the current $I^{db}_{i,j,k}$ and the voltage $V^{db}_{i,j,k}$ of the bypass diode can be expressed as follows:

$$I^{db}_{i,j,k} = I^{db}_0(e^{-V^{db}_{i,j,k}/V^{db}_t} - 1) \quad (6)$$

where I^{db}_0 and V^{db}_t are the bypass diode's saturation current and thermal voltage, respectively.

Obviously, the models of the N_s series-connected cells and bypass diode are coupled by the voltage $V_{i,j,k}$, which impose a complex computation. However, the bypass diode has an impact mainly at negative voltages, whereas it can be negligible at positive voltages. When some submodules are unevenly illuminated during partial shading, the negative voltage of the group of cells whose short current $I^{sc}_{i,j,k}$ is smaller than the current flowing through the submodule, can occur. Therefore, an alternative approach for decoupling the nonlinear and complex relationship between the group of cells and its antiparallel-connected bypass diode, as introduced in [9] and [10], is employed. Given the submodule current $I_{i,j,k}$, its voltage $V_{i,j,k}(I_{i,j,k})$ can be calculated as follows:

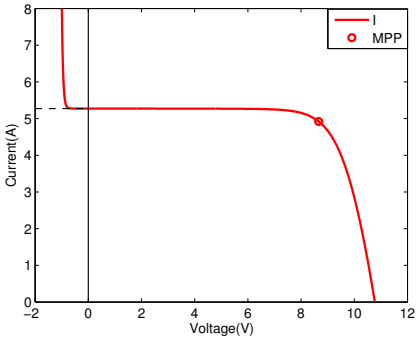

Fig. 3. An example of typical I-V characteristics for the submodule.

(1) If $0 \le I_{i,j,k} \le I^{sc}_{i,j,k}$, in this case the reverse current flowing through the bypass diode is negligible, the voltage $V_{i,j,k}$ and the current $I_{i,j,k}$ are equal to the voltage $V^g_{i,j,k}$ and the current $I^g_{i,j,k}$ of the group of cells, respectively. Therefore, given the current $I_{i,j,k}$, the voltage $V_{i,j,k}(I_{i,j,k})$ can be obtained by using the Newton-like method at a well-chosen initial iterative point $B\cdot ln(1+(I^{ph}_{i,j,k}-I_{i,j,k})/I^0_{i,j,k})-R^s_{i,j,k}\cdot I_{i,j,k}$ from the implicit relationship (2) by neglecting the current flowing through the parallel resistance R_p, where $B = N_s V^t_{i,j,k}(T_{i,j,k})A_{i,j,k}$. Empirically, that the maximum iteration number N^{Vmax}_{iter} is set to be 5, is enough for satisfying the precision requirement.

(2) If $I^{sc}_{i,j,k} < I_{i,j,k}$, in this case the current flowing through the PV submodule is assumed to be clipped at the short circuit current $I^{sc}_{i,j,k}$, the voltage is obtained from the explicit (6)

$$V_{i,j,k} = -V^{db}_t ln(\frac{I_{i,j,k} - I^{sc}_{i,j,k}}{I^{db}_0} + 1) \quad (7)$$

The setting of coefficients I^{db}_0 and V^{db}_t can be based on the characteristics of the diode [9]. In this study, I^{db}_0 and V^{db}_t are set to be $1.6\times10^{-9}(A)$ and $0.0468(V)$. As an example, an example of typical I-V characteristics for the submodule is shown in Fig.3.

III. Simulation Using Bisection Algorithm

It is easy to prove that the function $V_{i,j,k}(I_{i,j,k})$ is monotonically non-increasing on an interval $[0,\infty)$. That is to say , by defining $\Delta I_{i,j,k}$ and $\Delta V_{i,j,k}$ as the current increment of the submodule to the current $I_{i,j,k} \in [0,\infty)$ and the corresponding voltage increment to the voltage $V_{i,j,k}$, respectively, if $\Delta I_{i,j,k} \ge 0$ or $\Delta I_{i,j,k} \le 0$, then we have $\Delta V_{i,j,k} \le 0$ or $\Delta V_{i,j,k} \ge 0$.

Therefore, a bisection search method can be applied to solve the nonlinear equation $F_i(I_i) = 0$, where F_i is defined on an interval $[I^{min}_{i0}, I^{max}_{i0}]$. The left end point I^{min}_{i0} of the interval can be set to 0, i.e., $I^{min}_{i0} = 0$, meaning that the PV string circuit is open. In turn, the given voltage V_i should less than a sum of open-circuit voltages of all submodules as:

$$V_i < V^{max}_i = \sum_{j=1}^{N_m}\sum_{k=1}^{N_d} V^{oc}_{i,j,k}(G_{i,j,k}, T_{i,j,k}) \quad (8)$$

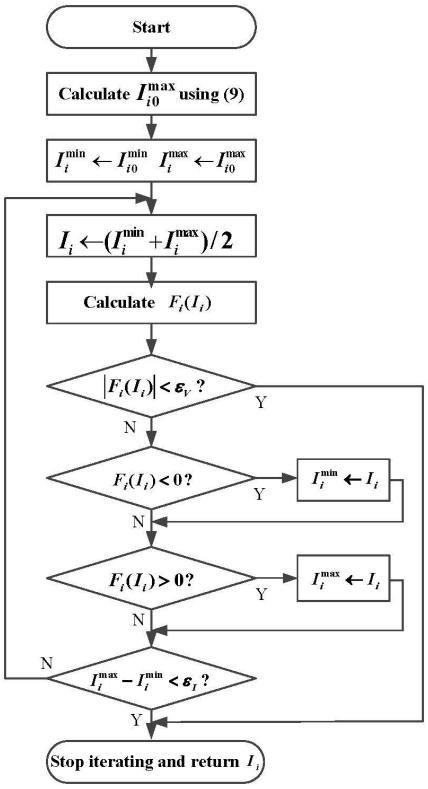

Fig. 4. Flow chart for the numerical computation of the string current I_i by using the bisection algorithm.

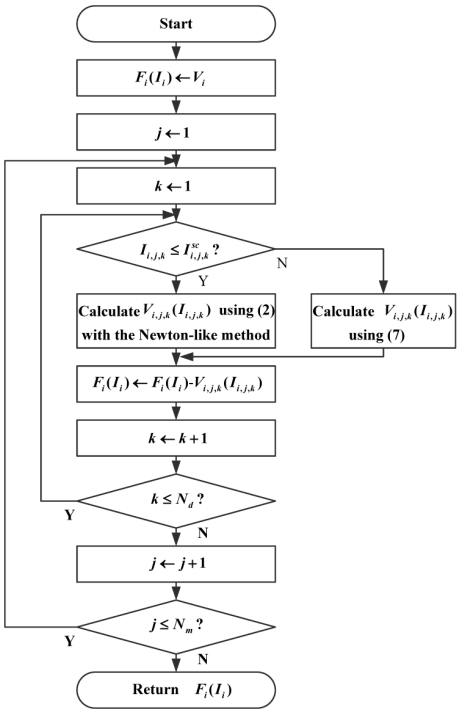

Fig. 5. Flow chart for the numerical computation of $F_i(I_i)$.

otherwise, we can give the solution directly as $I_i = 0$. The right end point I_{i0}^{max} of the interval can be set to the maximum value among the short-circuit currents as:

$$I_{i0}^{\max} = max(I_{i,1,1}^{sc}(G_{i,1,1}, T_{i,1,1}), \cdots, I_{i,j,k}^{sc}(G_{i,j,k}, T_{i,j,k}), \cdots, I_{i,N_m,N_d}^{sc}(G_{i,N_m,N_d}, T_{i,N_m,N_d})) \quad (9)$$

Consequently, the voltage V_i of the PV string with the current I_{i0}^{max} is less than V_i^{max}. Obviously, we have $F_i(I_{i0}^{min})F_i(I_{i0}^{max}) < 0$ when $V_i \in [0, V_i^{max})$.

The string current I_i is solved by means of the bisection algorithm detailed in the flow chart shown in Fig.4: given the PV array voltage V_A(or V_i), for any $i = 1, \cdots, N_p$, the algorithm numerically searches for the string current I_i such that the equation $F_i(I_i) = 0$ is satisfied. The flow chart of calculating $F_i(I_i)$ is shown in Fig.5. For identifying the global maximum of the output power of the PV array, the algorithm should be repeated varying the output voltage V_A(or V_i).

In the algorithm, ε_V and ε_I are the acceptable tolerances. Generally, that ε_V is set to be $0.01(V)$ and ε_I to be $0.001(A)$ is enough to simulation of the large-scale PV array. The number N_{iter} of iterations required to obtain an error smaller than ε_I should have:

$$N_{iter} > \frac{ln(I_{i0}^{\max}) - ln(\varepsilon_I)}{ln(2)} \quad (10)$$

Alternatively, the maximum number N_{iter}^{Imax} of iterations can be chosen as the convergence criterion. For the PV array simulation, that N_{iter}^{Imax} is set to be 20, is enough to obtain a satisfied tolerance because the maximum string current $I_{i0}^{\max}$ is less than 10(A).

Remarks. For the modeling method and solving technique, the accuracy, ease of implementation, robustness and calculation efficiency are key performance assessment indices. The proposed model has quite strong theoretical foundation for the use of bisection algorithm. The proposed simulation procedure is readily implemented, and the parameters and mathematical expressions are easy to manipulate by any researcher. Due to the use of separate circuit-voltage equations for all submodules, the proposed solving method presents the increased robustness and the reduced calculation time when compared with the methods using standard circuit simulation softwares and their improved methods using system of equations solved by the Newton-like methods, as highlighted in [17]. The convergence issue of calculating the voltage in (2) has be fully addressed because of the well-chosen initial iterative point of the iteration procedure. When a Newton-like method is employed to solve the system of equations consisting of (4) and (5), its computational complexity for each PV string simulation is $O(N_{iter}^{Newton} \times (N_m \times N_d)^3)$ because it involves inversion of a $N_m N_d \times N_m N_d$ Jacobian matrix, where N_{iter}^{Newton} is the maximum number of iterations. In contrast, the proposed computational method has the computational complexity of $O(N_{iter}^{Imax} \times N_{iter}^{Vmax} \times N_m \times N_d)$. The calculation time of solving the nonlinear implicit equation (2) using the Newtown-like algorithms for each submodule is almost constant because of the well-chosen initial iterative point and the limited maximum iteration number N_{iter}^{Vmax}. Therefore, the proposed method has significant improvement in the calculation efficiency when the PV system is large, namely, large $N_m \times N_d$ value. However, the accuracy of the proposed model can be acceptable, which is validated by the following simulation and experimental results. The step of the PV array voltage V_A is set to be $1(V)$ for finding

TABLE I
EXPERIMENTAL AIDE PV MODULE CHARACTERISTICS

Parameters	I_{sc}(A)	V_{oc}(V)	V_{mpp}(V)	I_{mpp}(A)
Values	9.228	45.278	36.635	8.700

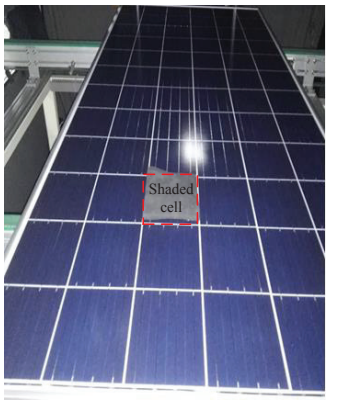

Fig. 6. Shading scenario of the module.

the MPPs of large PV strings by sweeping all specific array voltage values.

IV. EXPERIMENTAL AND SIMULATION RESULTS

A. Results for A PV Module Composed of Three Submodules Under Partial Shading Condition

To validate the accuracy of the proposed approach, the first simulation has been conducted by considering a multi-silicon PV module produced by Aide solar energy technology co., ltd. The module can be viewed as a submodule-based PV array with parameters $N_p = 1$, $N_m = 1$, $N_d = 3$ and $N_s = 24$. The experimental PV module characteristics at STC are shown in Table 1. The shading scenario is shown in Fig.6. One cell of the second submodule was shaded. The irradiance of the shaded cell was set to be $50W/m^2$. Both the I-V and P-V curves were recorded. The FS method [14], standing for the method using trust-region dogleg method without explicit Jacobian matrix, which can be available in Matlab through the *fsolve* function to the nonlinear equations (4) and (5), is utilized to compare the accuracy of simulations. Fig.7 and Fig.8 illustrate the I-V and the P-V characteristics obtained from the experimental data, the FS method and the proposed method, respectively.

The relative error of the generation power defined as

$$\delta_{p,v} = \frac{\left|P_{v,s} - P_{v,e}\right|}{P_{v,e}} \times 100\% \tag{11}$$

is used to evaluate the accuracy of the simulation methods [13]. The subscript v denotes a given voltage V_A. $P_{v,s}$ and $P_{v,e}$ are the simulated and experimental power at the voltage V_A, respectively. As illustrated in Fig.7 and Fig.8, the simulation results using the proposed method are very close to the experimental results when one bypass diode is active, while the results using the FS method are lower than the experimental

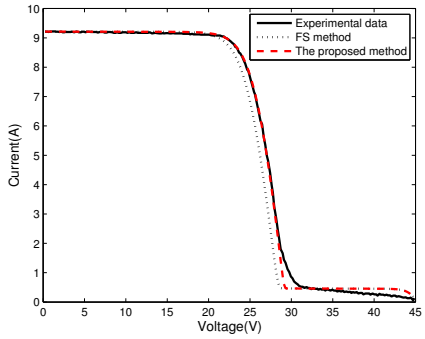

Fig. 7. Comparison of I-V characteristics among experimental data, the FS method and the proposed method.

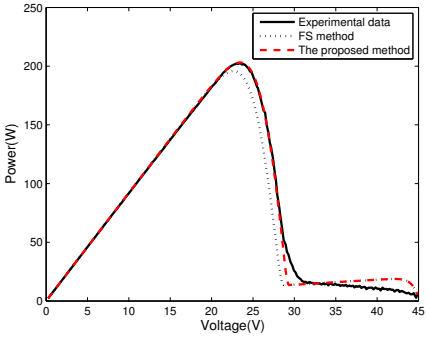

Fig. 8. Comparison of P-V characteristics among experimental data, the FS method and the proposed method.

data. The calculated mean relative errors of the generation power for the proposed method and the FS method are 1.58% and 6.88%, respectively. When all bypass diodes are inactive, the results of two simulation methods show large relative errors of the generation power. But the estimated current values of the proposed method are nearly identical with that of FS method. A possible explanation is that measure errors are relatively large when the currents flowing though all submodules are very low.

B. Results for a PV Array With the SP configuration Under Partial Shading Conditions

The second experiment was performed on the solar generation system installed on the rooftop of No.8 building, Fengxian district of East China University of Science and Technology (ECUST), Shanghai, China. The system is composed of 48 230W multi-silicon modules, a 12kW grid-connected inverter and an automatic weather station, as shown in Fig.9. The SP configuration parameters of the PV array are $N_p = 3$, $N_m = 16$, $N_d = 3$ and $N_s = 20$. After 5 years of operation, these modules have suffered severe power degradation. In addition, during last hours of the day, some modules are subjected to shadows produced by the wall. Therefore, by isolating one module temporarily from the array, real I-V characteristics of the module were first measured using an electronics load, and then five electrical model parameters were estimated.

Fig. 9. PV array installed at ECUST, Shanghai.

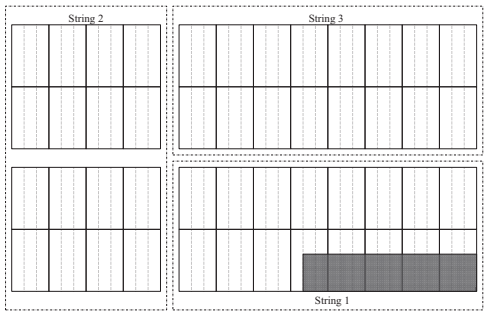

Fig. 10. Shading scenario 2.

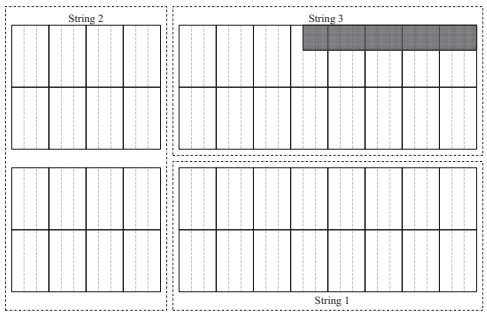

Fig. 11. Shading scenario 3.

Four experimental scenarios with different partial shading conditions are defined as:

Scenario 1: no shadow;

Scenario 2: four modules and two submodules in the string 1 are partially shaded by covering a rubber carpet on the 60% surface of the modules. Fig.10 shows the architecture of the PV array and the shading scenario;

Scenario 3: four modules and two submodules in the string 3 are partially shaded with horizontal shading profile produced by the wall, as shown in Fig.11;

Scenario 4: seven modules and one submodule in the string 3 are partially shaded with horizontal shading profile produced by the wall. Three modules and two submodules in the string 2 are also shaded. Fig.12 shows the shading scenario.

The voltage and current values of the PV array were read from the DC input values of the grid-connected inverter. The temperature and irradiance values were also read from the weather station. Fig.13 shows the irradiance level for each minute from 12:49 to 15:30 on April 13, 2017, excepting a few minutes for changing shading scenarios. Besides, we disconnected a module from the PV string to obtain the

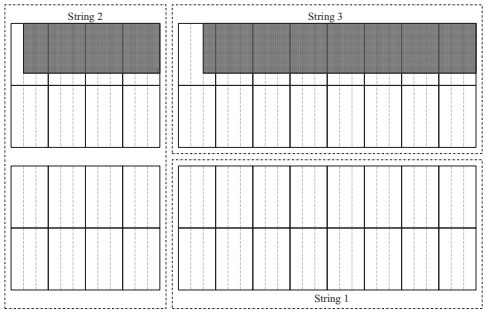

Fig. 12. Shading scenario 4.

module parameters. A direct current electronic load was used to capture a few of I-V characteristics of the module. Some key operating points, such as the short-circuit current, the open-circuit voltage and the MPP voltage and current, were extracted from the I-V characteristics. Then, the parameters of the submodules of the PV array were derived by using the key operating points and the approach in [21]. Finally, the extracted parameters were validated and adjusted using the I-V characteristics.

Fig.14 presents the estimated generation power obtained for each sampling point with the recorded irradiance level, the temperature value and the voltage given by the MPPT of the inverter. Four scenarios were performed on five different time intervals, as shown in Fig.14. It is observed from Fig.14 that the power curve estimated by using the proposed method follows with the real power curve. The calculated mean relative error of the generation power for the proposed method is 2.15%. Taking into account the uncertainties about the field data and nonuniform aging of the modules, the mean relative error value shows high simulation accuracy of the proposed method. An interesting observation in Fig.14 is that the generation power has significant increase at the middle of scenario 2 although the irradiance level gradually decreases. It can be inferred that the MPPT algorithm finally finds the maximum power point after minutes of calculation when the partial shading occurs suddenly.Therefore, if a model can infer the occurrence of partial shading and accurately estimate the generation power with the help of a monitoring system for a PV generation power plant, the global MPP could be theoretically obtained by performing the voltage sweeps on the PV array. It is our next work using the proposed model.

C. Simulation Approach to Evaluate the Electrical Mismatch Losses in Large-scale Photovoltaic Arrays With Nonuniform Aging

Nonuniform aging of the cells belonging to the same PV module can decrease the efficiency, reliability and lifetime of the PV plants and as a result the return on investment is reduced. With aging, nonuniform thermal and mechanical fatigue among the cells increase series resistances of the cells nonuniformly. The parallel resistances of the cells vary with the humidities and levels of corrosion at the corners of the cells [22]. Nonuniform cell delaminations involve inconsistent decreases of the short-circuit currents of the cells. Therefore,

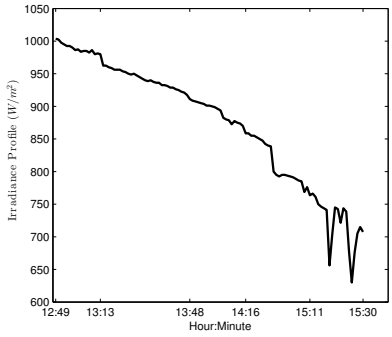

Fig. 13. Irradiance profile from 12:49 to 15:30 on April 13, 2017 at ECUST, Shanghai.

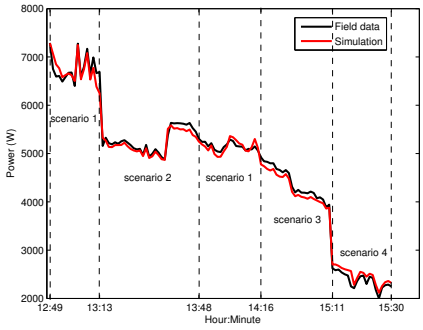

Fig. 14. Estimated power using the proposed model and the field power data

the nonuniform aging among the PV cells generates the different I-V characteristics. When the cells with these different I-V characteristics are interconnected, the mismatch loss arises. Moreover, as pointed out in [23], a closed-loop link between the nonuniform aging and the mismatching among the cells can exacerbate the power degradation of PV modules.

Although the impact of manufacturing I-V mismatch is negligible with the usual tolerance, as shown in [24] and [25], it is not clear if the same conclusion can be applied for the mismatch caused by the aging of modules. However, severe mismatches have been usually assumed in many research papers about control of mismatch power loss in PV arrays by using some reconfiguration strategies. In [26], currents at maximum power, voltages at maximum point, short circuit currents and open circuit voltages of modules have been assumed to follow Gaussian distributions with the standard deviations of 10% of their datasheet values. In [4], the short-circuit currents were uniformly chosen within the range between 30% and 90% of the datasheet value. Large deviations of the short-circuit currents have also shown in [27]. Obviously, the parameters dispersion of these papers is significantly larger than that of aged large-scale field PV arrays given in [28-33]. Moreover, modeling and simulation are the effective techniques commonly used to evaluate the mismatch losses caused by the nonuniform aging, and to assess the economical feasible of rearranging the modules in the large-scale PV plants. Several mathematical modeling approaches of the PV array with uneven mismatch conditions have been reviewed in [10]. However, very few of them are applicable to the large-scale PV arrays whose equivalent electrical models are characterized with numerous nonlinear equations bringing heavy computation burden. Therefore, the attention of this experiment was focused on providing a simulation approach to evaluate the electrical mismatch losses in large-scale PV arrays with reasonable degradation parameters. Some simple and easy reconfiguration strategies only by sorting modules in the middle and late lifetime of the PV arrays were evaluated.

A 250kWp series-parallel PV array with parameters $N_p = 50$, $N_m = 20$, $N_d = 3$ and $N_s = 20$ was simulated. Datasheet values of the module TSM-PD05.05(250W) were utilized to obtain the parameters of the submodule at the STC as $\tilde{V}^{oc} = 12.6667(V)$, $\tilde{I}^{sc} = 8.79(A)$, $\tilde{V}^{mpp} = 10.1(V)$ and $\tilde{I}^{mpp} = 8.27(A)$. The global number of modules is 1000. The degraded electrical parameters $V^{oc}_{i,j,k}$ and $I^{sc}_{i,j,k}$ of each submodule at the STC were assumed to follow Gaussian distributions as:

$$V^{oc}_{i,j,k} \sim N(\langle V^{oc}\rangle, 0.005\langle V^{oc}\rangle) \tag{12}$$

$$I^{sc}_{i,j,k} \sim N(\langle I^{sc}\rangle, 0.08\langle I^{sc}\rangle) \tag{13}$$

where $\langle V^{oc}\rangle = 0.98\tilde{V}^{oc}$ and $\langle I^{sc}\rangle = 0.92\tilde{I}^{sc}$ are the mean values of the parameters $V^{oc}_{i,j,k}$ and $I^{sc}_{i,j,k}$, respectively. The numerical coefficients such as 0.98 and 0.92, were chosen to simulate the degradation performance after about 15 years of operation. The sample values of $I^{sc}_{i,j,k}$ larger than the value of $\tilde{I}^{sc}$ were discarded. Larger standard deviation in the short-circuit current losses of the submodules indicates higher nonuniformity in heterogeneity submodules behavior affected by nonuniform aging processes.

The parameters $V^{mpp}_{i,j,k}$ and $I^{mpp}_{i,j,k}$ were generated by:

$$V^{mpp}_{i,j,k} = \tilde{V}^{mpp} \times \frac{V^{oc}_{i,j,k}}{\tilde{V}^{oc}} \times (1 - 0.02 \times r) \tag{14}$$

$$I^{mpp}_{i,j,k} = \tilde{I}^{mpp} \times \frac{I^{sc}_{i,j,k}}{\tilde{I}^{sc}} \times (1 - 0.05 \times r') \tag{15}$$

where r and r' are random numbers generated from an uniform distribution in the interval $[0, 1]$. The coefficients 0.02 and 0.05 were chosen to simulate the degraded fill factor (FF=$P^{mpp}/(V^{oc} \cdot I^{sc})$) due to the degradation of cell interconnections.

In all, using the stochastic random calculation method in [34], average losses in the parameters are theoretically as follows: V^{oc} : -2%, I^{sc} : -8%, P^{mpp} : -13%, and FF : -7%, respectively. In a sample of 3000 submodules, the total $P^{max}_{allsubmodules}$ of the maximum output power at the STC from each of the submodules is 213.96 kWp, denoting a power loss of about -14.4% with respect to the rated power value. The probability density functions of electrical parameters of all submodules are reported in Fig.15.

After extracting equivalent circuits parameters of all submodules using the approach in [21], we compared the output power of the PV array under the STC, with application of different sorting methods. It should be noticed that we only sorted the modules and the submodule configurations in the modules were not changed. The methods sorting modules by

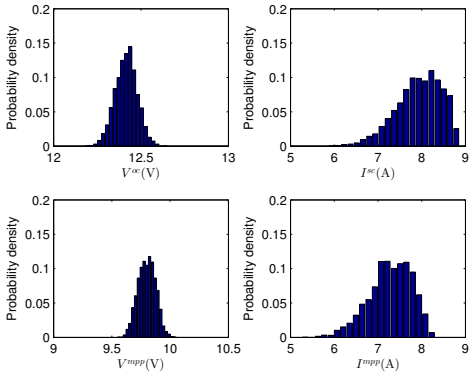

Fig. 15. Probability density functions of electrical parameters of submodules.

I^{sc} and I^{mpp} used the minimum short-circuit current and the minimum current at the maximum power point among the submodules belonging the same module, respectively. The methods sorting modules by P^{mpp} used the the maximum output power of the module from each of the submodules at the STC. The maximum output power P^{max}_{array} of the PV array sorting the modules according to the selected sorting parameters I^{sc}, I^{mpp} and P^{mpp} are 209.54 kWp, 209.60 kWp and 206. 98 kWp. Therefore, the resulting circuit mismatch (CMM) losses calculated by [35]:

$$CMM = \frac{P^{max}_{array}}{P^{max}_{allsubmodules}} - 1 \tag{16}$$

for the three methods are −2.066%, −2.038% and −3.262%. Obviously, sorting of modules according to I^{mpp} is the most efficient method to reduce circuit mismatch among the three methods. The performance of the method sorting of modules according to I^{sc} is very close to that of the method sorting of modules according to I^{mpp}.

In the non-sorted case the average value and standard deviation of the maximum output power of the PV array from 1000 simulation runs randomly placing the modules are 202.68 kWp and 0.164kWp, respectively. Therefore, compared to the non-sorted case, the maximum output power of the PV array of the methods sorting modules by I^{sc} and I^{mpp} increased by about 3.41%. However, the techno-economic analysis of these sorting techniques should consider the fee of the I-V measurements, labor cost of sorting the PV modules and electric price during the residual lifetime of the PV system [26,27].

This simulation codes were programmed by C language and compiled by GCC. The simulation calculations were performed on a laptop with a 2.4 GHz Intel CPU and a 16 GB memory. The running time of finding a current value by using the proposed bisection algorithm for a given voltage value was about 0.04($second$). The method using the Lambert-W function in [10] was also programmed by C language. The running time for the same simulation task using the method in [10] was about 0.063($second$), which is 1.5 times the calculation time of the proposed method. It is worth noting that the methods using the Lambert-W function, as shown in [7-10] and [36], are easy-to-use because of avoiding the need for iterative solution.

V. Conclusion

A simplified submodule-based model was introduced in the paper to simulate the nonlinear characteristics of the mismatched PV array equipped with the bypass diodes, dispensing with the need to resort to tedious cell-level modeling. Although the current flowing through the partially shaded PV submodule was not taken into consideration in the proposed model with the state of conducting the bypass diode, a simple, easy and robust computational method using the bisection search has been devised. However, its accuracy can also be acceptable, which has been validated and compared with other methods in some test examples. Moreover, the proposed simulation procedure can be utilized to evaluate the mismatch losses in aging PV arrays by arranging modules.

Acknowledgment

This work has been supported by the Chinese Scholarship Council (CSC). The work was also supported in part by the Natural Sciences and Engineering Research Council (NSERC) of Canada and the Saskatchewan Power Corporation (SaskPower). The authors would like to thank Aide solar energy technology co., ltd and Dr. Fangji Xie, Truewin Renewables Technology (Shanghai) Co., Ltd., for valuable support in providing the experimental data.

References

[1] N.D. Kaushika, and A. K. Rai, "An investigation of mismatch losses in solar photovoltaic cell networks," *Energy*, 2007, vol.32, no.5, pp.755-759.
[2] A. Chouder, and S. Silvestre, "Analysis model of mismatch power losses in PV systems," *ASME J. Solar Energy Engineering*, 2009, vol.131, p.024504.
[3] J. D. Bastidas-Rodriguez, C. A. Ramos-Paja, and A. J.Saavedra-Montes, "Reconfiguration analysis of photovoltaic arrays based on parameters estimation," *Simulation Modelling Practice and Theory*, 2013, vol.35, pp.50-68.
[4] Y. Hu, J. Zhang, J. Wu, et al, "Efficiency improvement of nonuniformly aged PV arrays," *IEEE Trans. Power Electron.*, 2017, vol.32, no.2, pp.1124-1137.
[5] J. W. Bishop, "Computer simulation of the effects of electrical mismatches in photovoltaic cell interconnection circuits," *Sol. Cells*, 1998, vol.25, no.1, pp.73-89.
[6] S. Silvestre, and A. Chouder, "Effects of shadowing on photovoltaic module performance," *Prog. Photovolt: Res. Appl.*, 2008, vol.16, pp.141-149.
[7] A. Dolara, G. C. Lazaroiu, S. Leva, and G. Manzolini, "Experimental investigation of partial shading scenarios on PV (photovoltaic) modules," *Energy*, 2013, vol.55, pp.466-475.
[8] G. Petrone, G. Spagnuolo, and M. Vitelli, "Analytical model of mismatched photovoltaic fields by means of Lambert W-function," *Sol. Energy Mater. Sol. Cells*, 2007, vol.91, pp.1652-1657.
[9] E. I. Batzelis, I. A. Routsolias, and S. A. Papathanassiou, "An explicit PV String model based on the Lambert W function and simplified MPP expressions for operation under partial shading," *IEEE Trans. Sustainable Energy*, 2014, vol.5, no.1, pp.301-312.
[10] J.D. Batidas, E. Franco, G.Petrone, C.A. Romas-paja, G. Spagnuolo, "A model of photovoltaic fields in mismatching conditions featuring an improved calculation speed," *Electr. Power Syst. Res.*, 2013, vol.96, pp.81-90
[11] G. Petrone, and C. A. Ramos-Paja, "Modeling of photovoltaic fields in mismatched conditions for Energy Yield Evaluations," *Electr. Power Syst. Res.*, 2011, vol.81, pp.1003-1013.

[12] S. Moballegh, and J. Jiang, "Modeling, prediction, experimental validations of power peaks of PV arrays under partial shading conditions," *IEEE Trans. Sustainable Energy*, 2014, vol.5, no.1, pp.293-300.
[13] J. Bai, Y.Cao, Y. Hao, Z. Zhang, S. Liu and F. Cao, "Characteristic output of PV systems under partial shading or mismatch conditions," *Solar Energy*, 2015, vol.112, pp.41-54.
[14] M. L. Orozco, J. M. Ramirez-Scarpetta, G. Spagnuolo, and C.A. Ramos-Paja, "A technique for mismatched PV array simulation," *Renewable Energy*, 2013, vol.55, pp.417-427.
[15] G. N. Psarros, E. I. Batzelis, and S. A. Papathanassiou, "Partial shading analysis of multistring PV arrays and derivation of simplified MPP expressions," *IEEE Trans. Sustainable Energy*, 2015, vol.6, no.2, pp.499-508.
[16] H. Patel, and V. Agarwal, "MATLAB-based modeling to study the effects of partial shading on PV array characteristics," *IEEE Trans. Energy Conv.*, 2008, vol.23, no.1, pp.302-310.
[17] E. I. Batzelis, P. S. Georgilakis, and S. A. Papathanassiou, "Energy models for photovoltaic systems under partial shading conditions: a comprehensive review," *IET Renew. Power Gener.*, 2015, vol.9, no.4, pp.340-349.
[18] P. Wang, H. Zhu, W. Shen, et al., "A novel approach of maximizing energy harvesting in photovoltaic systems based on bisection search theorem," in *Proc. 2010 Twenty-fifth Annu. IEEE Appl. Power Electron. Conf. Expo.*, Feb. 2010, pp.2143-2148.
[19] M. T. Ahmed, T. Goncalves, and M. Tlemcani, "Single diode model parameters analysis of photovoltaic cell," in *Proc. 2016 IEEE Int. Conf. Renew. Energy Res. Appl.*, Birmingham, London, Nov. 2016, pp.396-400.
[20] G. Liu, S. K. Nguang, and A. Partridge, "A general modeling method for I-V characteristics of geometrically and electrically configured photovoltaic arrays," *Energy Conv. and Manag.*, 2011, vol.52, pp.3439-3445.
[21] X. Feng, X. Qing, C. Y.Chung, et al., "A simple parameter estimation approach to modeling of photovltaic modules based on datasheet values," *ASME J. Solar Energy Engineering*, 2016, vol.138, p.051010.
[22] R. Doumane, M. Balistrou, P. O. Logerais, et al., "A circuit-based approach to simulate the characteristics of a silicon photovoltaic module with aging,"*ASME J. Solar Energy Engineering*, 2015, vol.137, no.2, p.021020.
[23] P. Manganiello, M. Balato, M. Vitelli, "A survey on mismatching and aging of PV modules: the closed loop," *IEEE Transactions on Industrial Electronics*, 2015, vol.62, no.11, pp.7276-7286.
[24] F. Spertino, J. S. Akilimali, "Are manufacturing I-V mismatch and reverse current key factors in large photovoltaic arrays? " *IEEE Transactions on Industrial Electronics*, 2009, vol.56, no.11, pp.4520-4531.
[25] A. M. Pavan, A. Tessarolo, N. Barbini, et al., "The effect of manufacturing mismatch on energy production for large-scale photovoltaic plants," *Solar Energy* , 2015, vol.117, pp.282-289.
[26] S. Shirzadi, H. Hizam, N I. A. Wahab, "Mismatch losses minimization in photovoltaic arrays by arranging modules applying a genetic algorithms," *Solar Energy*, 2014, vol.108, pp.467-478.
[27] M. Balato, L. Costanzo, M. Vitelli, "Reconfiguration of PV modules: a tool to get the best compromise between maximization of the extracted power and minimization of localized heating phenomena," *Solar Energy*, 2016, vol.138, pp.105-118.
[28] A. Skoczek, T. Sample, E. D. Dunlop, "The results of performance measurements of field-aged crystalline silicon photovoltaic modules," *Progress in Photovoltaic: Research and Applications*, 2009, vol.17, pp.227-240.
[29] P. Sanchez-Friera, M. Piliougine, J. Pelaez, et al., "Analysis of degradation mechanisms of crystalline silicon PV modules after 12 years of operation in southern Europe. *Progress in Photovoltaic: Research and Applications*, 2011, vol.19, pp.658-666.
[30] A. Ndiaye, C. M. Kebe, A. Charki, et al., "Degradation evaluation of crystalline-silicon photovoltaic modules after a few operation years in a tropical environment," *Solar Energy* , 2014, vol.103, pp.70-77.
[31] A. Limmanee, S. Songtrai, N. Udomdachanut, et al., "Degradation analysis of photovoltaic modules under tropical climatic conditions and its impacts on LCOE," *Renewable Energy*, 2017, vol.102, pp.199-204.
[32] A. Pozza A, T. Sample, "Crystalline silicon PV module degradation after 20 years of field exposure studied by electrical tests, Electroluminescence, and LBIC," *Progress in Photovoltaic: Research and Applications*, 2016, vol.24, pp.368-378.
[33] D. C. JordanC, S. R. Kurtz, "Photovoltaic degradation rates - an analytical review," *Progress in Photovoltaic: Research and Applications*, 2013, vol.21, pp.12-29.
[34] F. Iannone, G. Noviello, and A. Sarno, "Monte Carlo techniques to analyse the electrical mismatch losses in large-scale photovoltaic generators," *Solar Energy*, 1998, vol.62, no.2 pp.85-92.
[35] W. Hermann, S. Kammer, and U. Yusufoglu, "Circuit losses in PV arrays caused by electrical mismatch of PV modules - impacts of temperature gradients and a variation of irradiance," in *28th European Photovoltaic Solar Energy Conference and Exhibition*, pp.4127-4131.
[36] J. Accarino, G. Petrone, C.A. Ramos-Paja, and G. Spagnuolo, "Symbolic algebra for the calculation of the series and parallel resistances in PV module model," in *Proc. 4th Int. Conf. Clean Elect. Power*, Alghero, Italy, Jun. 2013, pp.62-66.